J. Cell. Mol. Med. Vol 14, No 5, 2010 pp. 1166-1179

Moesin-dependent cytoskeleton remodelling is associated with an anaplastic phenotype of pancreatic cancer

Ivane Abiatari [a], Irene Esposito [b, c], Tiago De Oliveira [a], Klaus Felix [d], Hong Xin [a], Roland Penzel [e], Thomas Giese [f], Helmut Friess [a], Jörg Kleeff [a, g, *]

[a] Department of General Surgery, Technische Universität München, Ismaningerstrasse 22, 81675, Munich, Germany
[b] Institute of Pathology, Technische Universität München, Munich, Germany
[c] Institute of Pathology, Helmholtz Zentrum München, Neuherberg, Germany
[d] Department of General Surgery, University of Heidelberg, Heidelberg, Germany
[e] Department of Pathology, University of Heidelberg, Heidelberg, Germany
[f] Department of Immunology, University of Heidelberg, Heidelberg, Germany
[g] Center of Cancer Systems Biology, Department of Medicine, Caritas St. Elizabeth's Medical Center, Tufts University School of Medicine, Boston, MA, USA

Received: February 2, 2009; Accepted: April 3, 2009

Abstract

Cell motility is controlled by the dynamic cytoskeleton and its related proteins, such as members of the ezrin/radixin/moesin (ERM) family, which act as signalling molecules inducing cytoskeleton remodelling. Although ERM proteins have been identified as important factors in various malignancies, functional redundancy between these proteins has hindered the dissection of their individual contribution. The aim of the present study was to analyse the functional role of moesin in pancreatic malignancies. Cancer cells of different malignant lesions of human and transgenic mice pancreata were evaluated by immunohistochemistry. For functional analysis, cell growth, adhesion and invasion assays were carried out after transient and stable knock-down of moesin expression in pancreatic cancer cells. *In vivo* tumourigenicity was determined using orthotopic and metastatic mouse tumour models. We now show that moesin knock-down increases migration, invasion and metastasis and influences extracellular matrix organization of pancreatic cancer. Moesin-regulated migratory activities of pancreatic cancer cells were in part promoted through cellular translocation of β-catenin, and re-distribution and organization of the cytoskeleton. Analysis of human and different transgenic mouse pancreatic cancers demonstrated that moesin is a phenotypic marker for anaplastic carcinoma, suggesting that this ERM protein plays a specific role in pancreatic carcinogenesis.

Keywords: moesin • pancreatic ductal adenocarcinoma • anaplastic cancer • cytoskeleton • β-catenin • extracellular matrix

Introduction

Pancreatic cancer is characterized by numerous genetic and epigenetic alterations [1, 2] resulting in high invasiveness, early metastasis and poor prognosis, with an overall 5-year survival rate of less than 5% [3]. The fatal nature of pancreatic cancer stems from its propensity to rapidly disseminate into the lymphatic system, spread along nerves and metastasize to distant organs [4]. The most common malignancy of the pancreas is pancreatic ductal adenocarcinoma (PDAC), which accounts for 85–90% of all pancreatic tumours. Pancreatic anaplastic carcinoma (PAC) is a relatively rare neoplasm, characterized by pleomorphic or sarcomatoid tumour growth that also harbours k-ras mutations in a high percentage and shows a cytokeratin expression profile that suggests a similar origin as PDAC [5]. However, due to the low incidence of PAC, the exact molecular characteristics and the clinical outcome of this malignancy (especially in comparison with PDAC) are not known.

Membrane-organizing extension spike protein (moesin / MSN) is a member of the highly related ERM (ezrin/radixin/moesin)

*Correspondence to: Jörg KLEEFF, M.D.,
Department of Surgery, Klinikum rechts der Isar,
Technische Universität München,
Ismaningerstr. 22, 81675 Munich, Germany.
Tel.: +49 (89) 4140 5098
Fax: +49 (89) 4140 4870
E-mail: kleeff@gmx.de

doi:10.1111/j.1582-4934.2009.00772.x

actin-binding protein family. ERM proteins act as linkers between the actin cytoskeleton and the plasma membrane [6], and regulate cell morphology, motility and other processes that are implicated in tumourigenesis [7]. The structural-functional role of moesin has been assessed in epithelial cell polarity and cortical actin congregation [8, 9]. Moesin has also been implicated in epithelial-to-mesenchymal transition (EMT) [7]. Previously, expression of ezrin has been associated with the aggressiveness of pancreatic and endometrial cancers [10–12], and enhanced expression of ezrin/radixin/moesin has been associated with poor survival of pancreatic cancer patients [13, 14]. In contrast, another family member, merlin, has been identified as a tumour suppressor [15, 16]. Nevertheless, ERM proteins are considered to be functionally redundant when co-expressed in mammalian cells [17], and there are insufficient data regarding the specific role of moesin in carcinogenesis.

Materials and methods

Patients and tissue collection

Seventy PDAC and eight PAC tissue samples were obtained from patients (median age 62.5 years; range 41–78) who underwent pancreatic resections at the University Hospital of Heidelberg (Germany). Ten normal human pancreatic tissue samples were obtained from previously healthy individuals through an organ donor program (median age 45 years; range 20–74 years). All studies were approved by the Ethics Committee of the University of Heidelberg. Written informed consent was obtained from all patients.

Cell culture

Pancreatic cancer cell lines: Aspc1, BxPc3, Capan1, Colo375, MiaPaca2, Panc-1, SU8686 and T3M4 were routinely grown in RPMI medium supplemented with 10% foetal calf serum (FCS), 100 U/ml penicillin, and 100 μg/ml streptomycin. Cells were maintained at 37°C in a humid chamber with 5%CO_2 and 95% air atmosphere. Two primary PDAC cell lines were freshly isolated from human pancreatic cancer tissues and were used between the third and fifth passage. Human Pancreatic stellate cells where isolated from pancreatic cancer tissues using the outgrowth method as described previously [18].

Real-time quantitative polymerase chain reaction (QRT-PCR)

All reagents and equipment for mRNA and cDNA preparation were purchased from Roche (Roche Applied Science, Mannheim, Germany). mRNA was prepared by automated isolation using the MagNA Pure LC instruments and isolation kit I (for cells) and kit II (for tissues). RNA was reverse transcribed into cDNA using the 1st Strand cDNA Synthesis Kit for RT-PCR (AMV) according to the manufacturer's instructions. QRT-PCR was performed with the Light Cycler Fast Start DNA SYBR Green kit as described previously [19]. The number of specific transcripts was normalized to the housekeeping gene cyclophilin B (CPB) and presented as copies/10,000 copies of CPB. All primers were obtained from Search-LC (Heidelberg, Germany).

Immunohistochemistry

Paraffin-embedded tissue sections (2–3 μm thick) were deparaffinized and rehydrated. Thereafter, slides were placed in washing buffer. Antigen retrieval was performed by microwaving the tissue sections in 10 mM citrate buffer for 10 min. Sections were incubated with normal goat serum (DAKO Corporation, Carpinteria, CA, USA) for 45 min. to block the nonspecific binding sites, and then incubated with mouse monoclonal moesin (Serotec GmbH, Dsseldorf, Germany), rabbit polyclonal moesin (Abcam, Cambridge, UK) (for mice tumours), mouse monoclonal ezrin (Abcam), goat polyclonal radixin (Santa Cruz Biotech, Santa Cruz, CA, USA), or rabbit polyclonal phospho-ezrin (Thr567)/radixin (Thr564)/moesin (Thr558) (Cell Signaling Technology, Danvers, MA, USA) antibodies. After washing, slides were incubated with secondary antibodies (goat anti-mouse or goat anti-rabbit labelled polymer, HRP antibodies, DAKO Corp., and donkey anti-goat HRP diluted 1:500 from Santa Cruz Biotech), for 45 min. at room temperature (RT). Thereafter, tissue sections were incubated with 100 μl of the DAB+ Chromogen (DAKO Corp.).

Immunoblot analysis

Cell culture monolayers were washed twice with ice-cold phosphate buffer solution (PBS) and lysed with lysis buffer (50 mM Tris-HCl, 100 mM NaCl, 2 mM EDTA, 1% SDS) containing a protease inhibitor cocktail (Roche), 500 mM sodium fluoride and 100 mM sodium orthovanadate (for phosphorylated proteins). Cell lysates (30 μg/lane were separated on SDS-polyacrylamide gels (Invitrogen, Karlsruhe, Germany) and electroblotted onto nitrocellulose membranes. Membranes were then incubated in blocking solution (5% nonfat milk/1.5% BSA in 20 mM Tris-HCl, 150 mM NaCl, 0.1% Tween-20), followed by incubation with the indicated antibodies at 4°C overnight. After washing, membranes were incubated with HRP-conjugated secondary antibodies for 1 hr at RT. Antibody detection was performed by an enhanced chemiluminescence reaction. Densitometry analysis of the blots was performed by ImageJ software (National Institutes of Health, Bethesda, MD, USA). Blot of the test protein was normalized to the blot of the control protein, which was used as equal loading.

Immunofluorescence analysis

Frozen tissue sections (4–5 μm thick) were air dried and fixed with ice-cold acetone for 2 min. (RT). Cells were grown in complete medium overnight in 10-well chambers, washed with PBS, fixed with 4% formaldehyde/PBS for 20 min. at RT, incubated in ice-cold methanol for 5 min. (RT), and subsequently incubated in acetone for 2 min. (RT). Slides were then incubated overnight with primary antibodies at 4°C. After that, slides were washed with PBS and incubated with fluorescent-labelled secondary antibodies for 1 hr (RT), washed, and incubated with Alexa Fluor® 488 phalloidin (Molecular Probes, Inc., Eugene, OR, USA). Slides were then mounted with DAPI and anti-fading medium (Gel/mount™, Abcam, Cambridge, UK). Confocal microscopic analysis was performed using the Spectral Confocal Microscope Leica TCS SL (Leica Microsystems GmbH, Heidelberg, Germany).

Transient and stable transfection

For transient transfection, specific validated and control siRNAs were used (Qiagen, Hilden, Germany). Five μg siRNA/well were transfected using RNAi-Fect™ (Qiagen) as transfection agent in 6-well plates. Expression analysis and functional experiments were performed after 96 hrs. shRNA for moesin (Top primer- 5′-CAC CGG GTC TCA ACA TCT ATG AGC AGA ATC GAA ATT CTG CTC ATA GAT GTT GAG AC-3′) and control (scrambled) shRNA was cloned as hairpin oligonucleotide into the pLenti4/BLOCK-iT™-DEST vector and lentiviral package (Invitrogen), according to the manufacturer's instructions. Stable clones were obtained after selection with Zeocin™.

In vitro adhesion assays

Matrigel Basement Membrane Matrix, Phenol-Red Free (BD Biosciences, Bedford, MA, USA) was diluted 1:10 in compete cell culture medium, and added to 24-well tissue culture plates to solidify overnight [20]. 5×10^4 cells/well were seeded and incubated in a 37°C humid chamber. At indicated time-points, cells were washed twice with PBS and counted manually in high power optical fields.

In vitro invasion assays

Assays were performed in a BD Biocoat Matrigel InvasionChamber with 8-μm pore size (BD Biosciences, Heidelberg, Germany) according to the manufacturer's instructions [18]. Matrigel was rehydrated with 500-μl serum-free cell culture medium and incubated in 37°C, 5% CO_2 atmosphere for 2 hrs 5×10^4 cells/ml were added to the top chamber and incubated for 24 hrs. Cells adhering to the lower surface were fixed with 75% methanol mixed with 25% acetone and stained with 1% toluidine blue. The whole membrane was scanned and the invading cells were counted. The invasion index was expressed as the ratio of the per cent invasion of silenced cells over the per cent invasion of the control cells.

Wound healing assays

An artificial 'wound' was created using a 10-μl pipette tip on confluent cell monolayers in 6-well culture plates as described previously [21]. Quantification of 'wound' closure was carried out by counting the number of cells in the 'wound' area after 8 hrs and expressed as the average per three optical fields.

Anoikis assay

Cells were plated at a density of 1×10^5 cells per well in 12-well plates coated with 2 ml of a 20 mg/ml polyHEMA (polyhydroxyethylmethacrylate)/ethanol solution [22]. After incubation for 72 hrs, the cell suspension was collected, dissolved in 1:4 water-diluted binding buffer and 5-μl annexin V-FITC (human annexin kit, Bender MedSystems, Burlingame, CA, USA) was added. Cell viability was detected by FACS after adding 10 μl of the 20 μg/ml propidium iodide solution.

In vivo tumour models

In vivo mouse tumourigenicity models and analysis of proliferation capacity and microvessel density of orthotopic tumours were performed using athymic Crl:NU/NU-Foxn1^{nu} (NU/NU) nude mice as described previously [20]. For the *in vivo* metastasis model, 1×10^6 cells in 100 μl PBS were injected into the portal vein of athymic nude mice using a 26-gauge needle. After 1 month, animals were sacrificed and snap-frozen livers analysed. All animal studies were approved by the State Review Board. Tissue sections of pancreatic tumours from *Pdx*$^{-Cre}$*;CLEG2;Kras*^{G12D}, *Pdx*$^{-Cre}$*;CLEG2* [23] and *P48*$^{+/Cre}$*;LSL-Kras*^{G12D} [24] transgenic mice models were evaluated for morphology and expression of moesin.

Statistical analysis

All experiments were performed in biological triplicates unless indicated otherwise. Results were expressed as mean ± standard error of the mean (S.E.M.) unless indicated otherwise. For statistical analysis, the Student's t-test was used. Significance was defined as $P < 0.05$.

Results

High expression of moesin in PAC and absent expression in PDAC

Characterization of ERM proteins in pancreatic tissues revealed strong expression of Ezrin in small ducts and centroacinar cells of the normal pancreas (Fig. 1A-1) and in cancer cells of PDAC (Fig. 1A-2). Ezrin was also present in some cells of PAC (Fig. 1A-3). Expression of radixin was observed in the cancer cells of PDAC and PAC tissues, but to a comparably lesser extent (Fig. 1A-4, 5). Expression of moesin was faintly detectable in normal pancreatic tissues (Fig. 1B-1) but present in fibroblasts/stellate cells and inflammatory cells of chronic pancreatitis (CP) tissues (Fig. 1B-2). Expression of moesin (and to a lesser extent of ezrin and radixin) in cultured pancreatic stellate cells as well as in peripheral blood mononuclear cells was also confirmed by QRT-PCR (Fig. 1C-3). None of the tested PDAC tissues ($n = 70$) showed positive staining for moesin in the cancer cells (Fig. 1B-3–5, 8). In contrast, moesin was found to be abundant in the neoplastic cells of PAC ($n = 8$) (Fig. 1B-6, 7), which was also confirmed by confocal microscopy, demonstrating to some extent co-localization with actin (Fig. 1B-9).

We analysed one case of PAC with associated PanIN lesions [25]. Interestingly, anaplastic cancer cells demonstrated strong expression of moesin (Fig. 1C-1), whereas PanIN lesions of the same tissue were generally negative for moesin (Fig. 1C-2), except for the PanIN lesions with direct association to anaplastic cells (data not shown).

All eight tested pancreatic cancer cell lines strongly expressed moesin at the mRNA and protein level, and most of them also

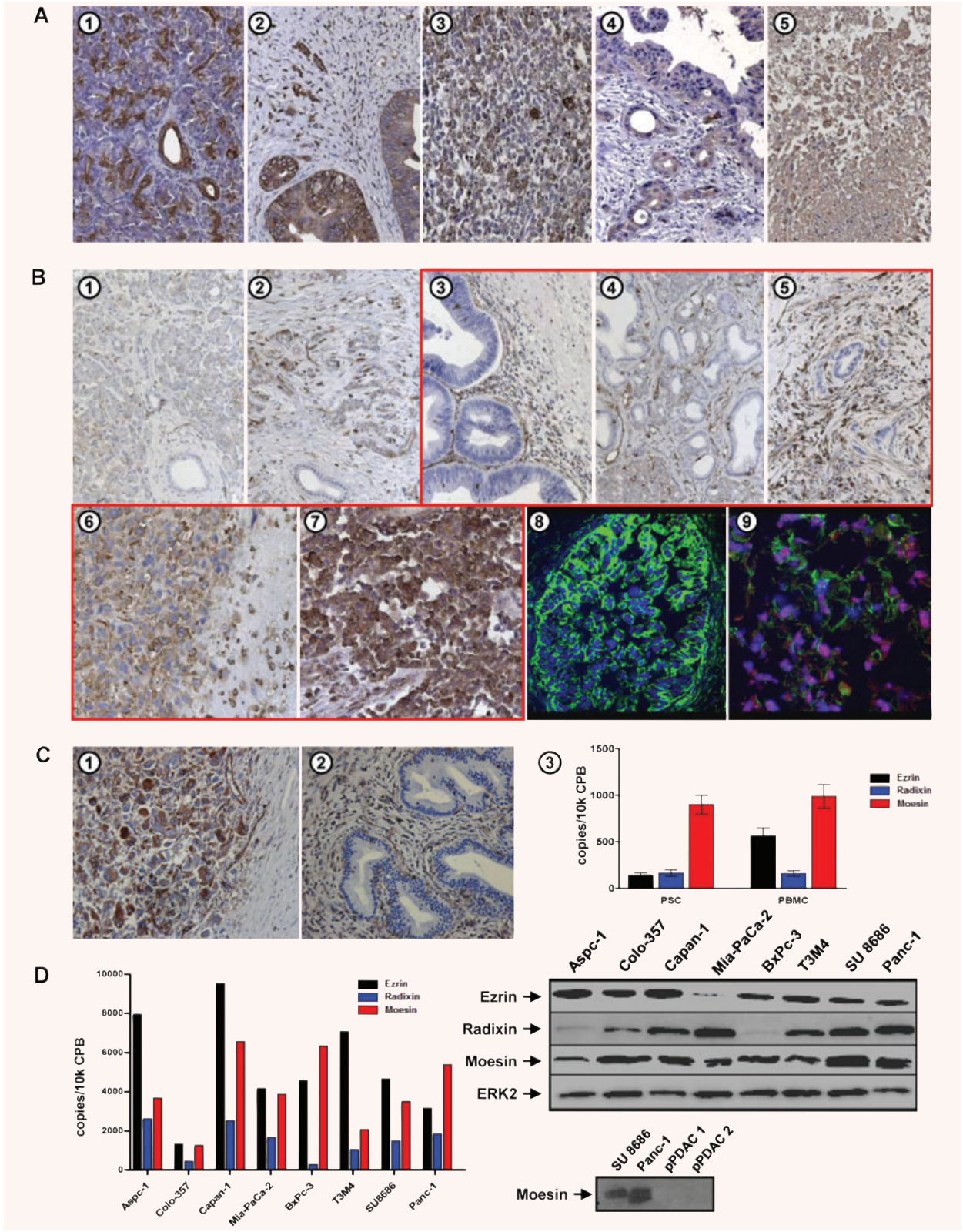

Fig. 1 High expression of moesin in PAC and loss of expression in PDAC. (**A**) Immunohistochemical staining of normal pancreas (1), PDAC (2) and PAC (3) samples using a specific ezrin antibody and of PDAC (4) and PAC (5) samples, using a specific radixin antibody (20× magnification). (**B**) Immunohistochemical staining of normal pancreas (1), CP (2), PDAC (3–5) and PAC (6, 7) samples using a specific moesin monoclonal antibody (20× magnification). Immunofluorescence confocal microscopy staining of PDAC (8) and PAC (9) tissues using the moesin antibody (red). Note actin (green), and nuclear (blue) DAPI counterstaining. (**C**) Immunohistochemical staining of PAC (1) containing PanIN lesions (2) with a specific moesin antibody (20× magnification). (3) QRT-PCR data of ezrin/radixin/moesin expression in pancreatic stellate cells (PSC) and peripheral blood mononuclear cells (PBMC). (**D**) QRT-PCR showing expression of ezrin/radixin/moesin (left panel), and immunoblot analysis showing expression of ezrin/radixin/moesin in eight cultured pancreatic cancer cell lines (right panel), as well as in two primary pancreatic cancer cell lines (pPDAC1; pPDAC2; lower panel).

expressed ezrin and radixin (Fig. 1D). Since freshly isolated primary pancreatic cancer cells (pPDAC; passage 2–4) displayed absence of moesin mRNA and protein expression (Fig. 1D, lower panel), which is in line with the results obtained from pancreatic tissues, moesin expression might be regained under long-term culture conditions in PDAC cells.

Silencing of moesin results in decreased adherence and increased invasion and migration

For functional assessment of moesin, transient RNAi transfection of Panc-1 and SU8686 pancreatic cancer cell lines was utilized. Immunoblot analysis demonstrated reduced moesin expression after 96 hrs of MSN RNAi compared to control RNAi (Figs 2A, 3A and 4A).

Matrigel adhesion assays revealed significantly decreased adherence following moesin silencing in SU8686 cells ($P < 0.05$), while there was only a tendency for reduced adhesion in moesin silenced Panc-1 cells (Fig. 2B). In contrast, there was a 1.8 ± 0.15 ($P < 0.05$) fold increased invasive capacity of moesin RNAi-transfected Panc-1 cells and an 8.2 ± 1.5 ($P < 0.05$) fold increased invasive capacity of moesin RNAi-transfected SU8686 cells compared to control RNAi-transfected cells (Fig. 2C). Similarly, analysing the migration capacity, there was a 3-fold increased migration for moesin silenced Panc-1 (93.6 ± 8.5) and a 2.8-fold increased migration for moesin silenced SU8686 cells (46.1 ± 4.9) (Fig. 2D-1, 2) compared to controls.

Moesin controls the expression pattern of β-catenin without inducing cadherin switch

To identify whether moesin mediated migratory changes of pancreatic cancer cells are related to EMT, we studied the expression of various EMT markers [26] upon down-regulation of moesin in pancreatic cancer cells. Immunoblotting revealed down-regulation of N-cadherin in moesin RNAi-transfected SU8686 cells. In contrast, in Panc-1 cells the expression of N-cadherin even under control conditions was not detectable (Fig. 3A). There were no significant relation between the expression of other EMT-related molecules and moesin expression in Panc-1 and SU8686 cell lines (Fig. 3A). Since we did not observe a cadherin switch in moesin transfected Panc-1 and SU8686 cells, we analysed the expression pattern of β-catenin, as an important factor in EMT [27]. β-catenin displayed a membranous co-expression with moesin in wild-type and control transfected Panc-1 and SU8686 pancreatic cancer cells (Fig. 3B). However, moesin RNAi transfected cells displayed reduced membranous localization of β-catenin (Fig. 3B), even though there was no change in expression levels of β-catenin between control and moesin silenced cancer cells (data not shown).

Generation of cell lines stably expressing moesin shRNA

In order to better assess the biological role of endogenous moesin, we stably suppressed moesin expression by lentiviral vector-based transduction of specific shRNA in SU8686 pancreatic cancer cells. Immunoblotting revealed significant down-regulation of protein expression ($-84.5 \pm 1.6\%$) in moesin shRNA-transfected cells (Lv-MSN) compared to control shRNA transfected cells (Fig. 4A). Differences in the expression of cellular moesin could also be confirmed by immunofluorescence confocal microscopy, where expression of moesin in Lv-MSN cells was below the level of detection (Fig. 4B).

Since moesin has been implicated in metastatic activities of numerous malignancies [28], we investigated the role of moesin in anoikis. Lv-MSN cells demonstrated high viability in a non-adherent environment with a significantly lower number of apoptotic cells compared to wild-type and Lv-control cells after 72 hrs (Fig. 4C).

Next, we investigated actin organization, upon serum starvation and 10 min. serum activation in the presence or absence of moesin using phalloidin staining of filamentous actin. Lv-control cells displayed apical actin organization, with the formation of cortical and transverse stress fibres (Fig. 4D-1). Moreover, actin expression was associated with stably organized adherence junctions in these cells (Fig. 4D-2). Lv-MSN cells displayed strong accumulation of filamentous actin, with intense formation of cortical stress fibres (Fig. 4D-4), which was related to disruption of adherence junction stability and formation of membrane protrusion and filopodia (Fig. 4D-5). Furthermore, fluorescent staining of

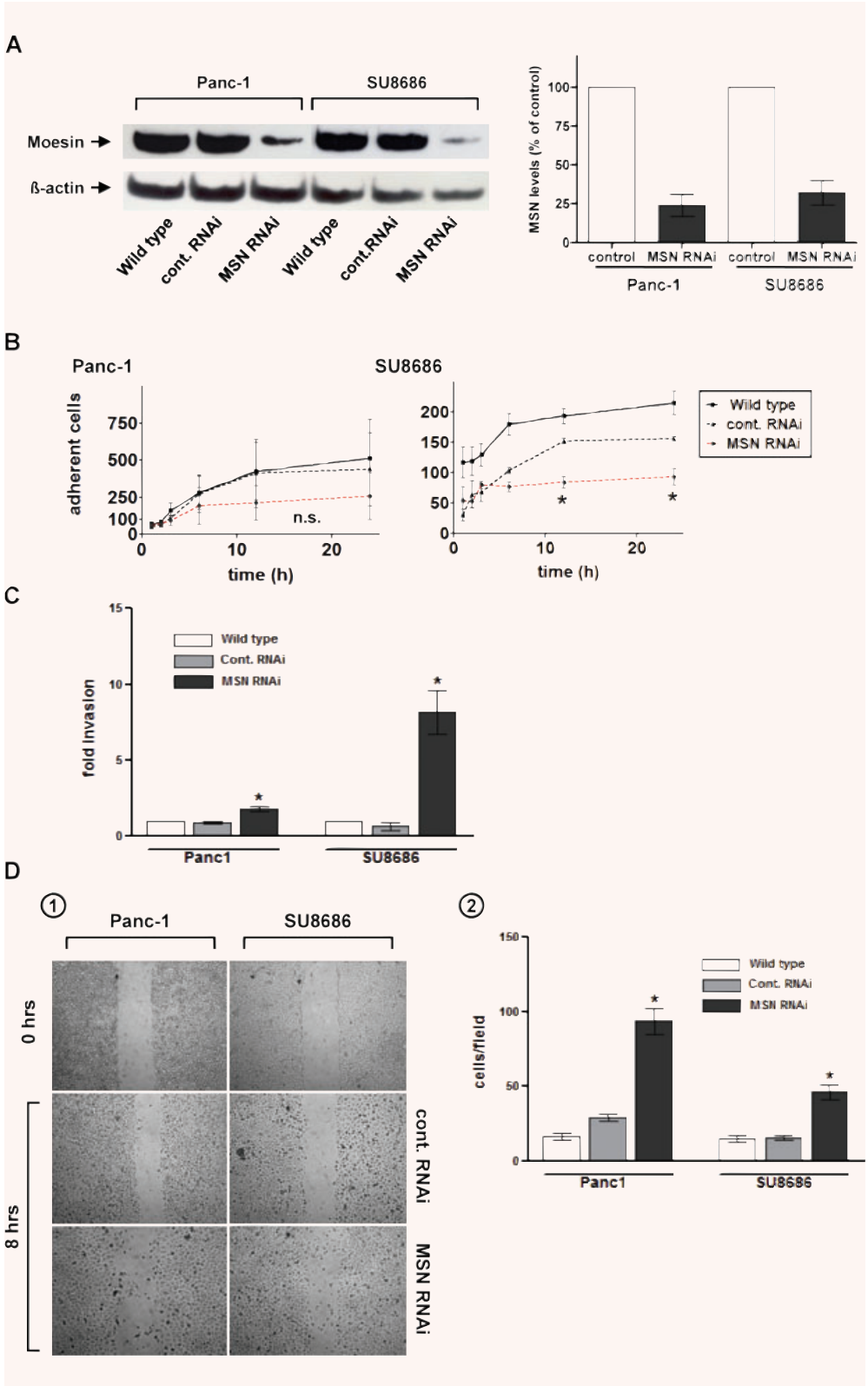

Fig. 2 Moesin promotes adhesion and reduces invasion and migration. (**A**) Immunoblot showing transient down-regulation of moesin in Panc1 and SU8686 pancreatic cancer cell lines compared to controls using siRNA transfection (left) and densitometric quantification of moesin down-regulation in these cells (right). Data are shown as mean ± S.E.M. (**B**) Quantification of adhesion assay of Panc1 and SU8686 cells after moesin silencing. Adherent cells were counted under the microscope and are expressed as the mean ± S.E.M. per three optical high-power fields. $*P < 0.05$ compared to control cells. (**C**) Quantification of two-chamber invasion assays of Panc1 and SU8686 cells after moesin silencing. Data are shown as mean ± S.E.M. $*P < 0.05$ compared to control cells. **D:** Wound healing assay with Panc1 and SU8686 control and moesin RNAi cells (1). Quantification of Panc1 and SU8686 cells migrating into a defined wound area after 8 hrs. Cells in four defined areas per group per experiment were quantified (2). Data are shown as mean ± S.E.M. $*P < 0.05$ compared to control cells.

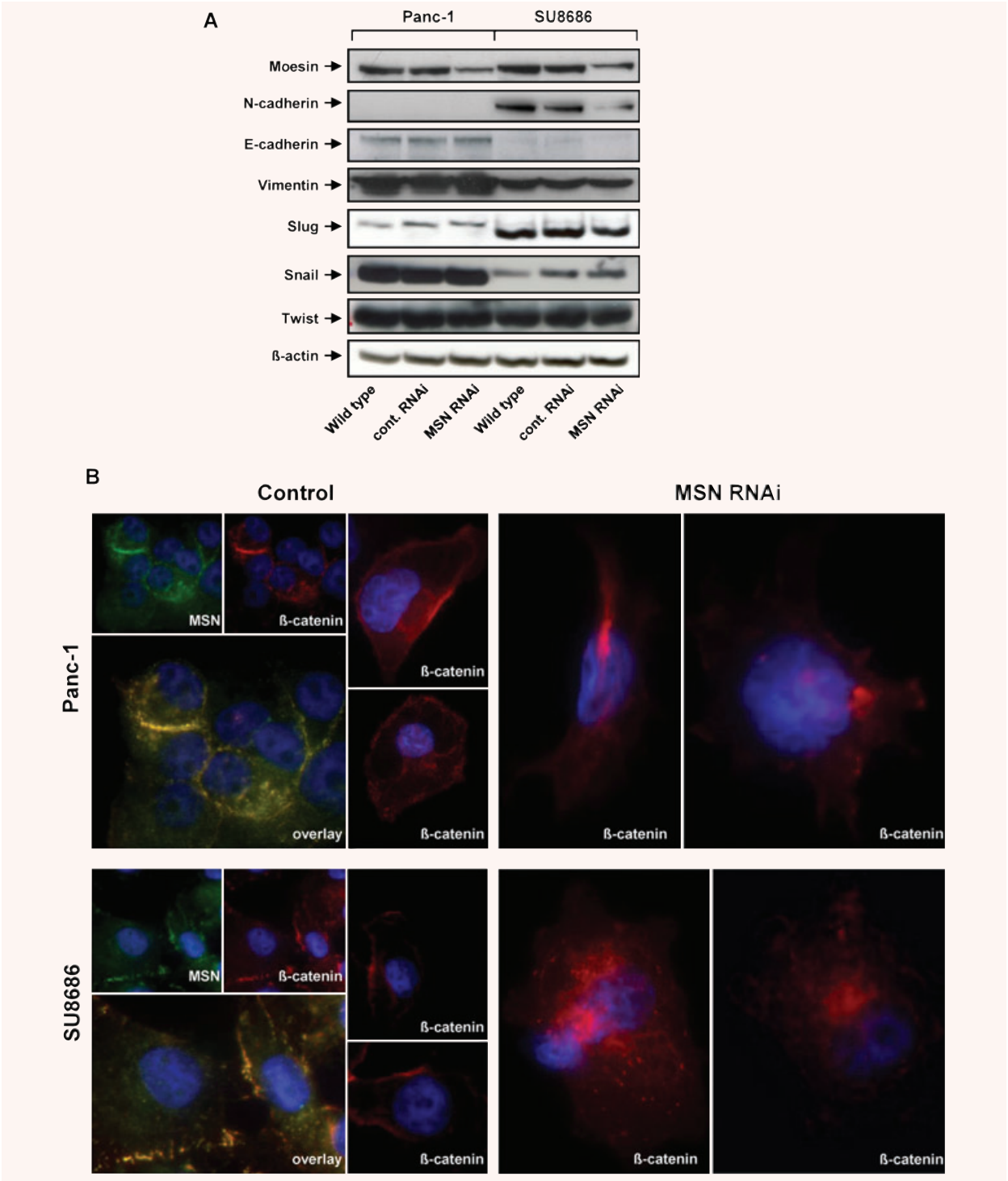

Fig. 3 Moesin influences the localization of β-catenin without inducing cadherin switch. (**A**) Immunoblot analysis showing expression of N-cadherin, E-cadherin, vimentin, slug, snail and twist in Panc1 and SU8686 pancreatic cancer cell lines after moesin siRNA silencing. (**B**) Immunofluorescence analysis of control and MSN siRNA transfected Panc1 and SU8686 cells showing moesin (green), β-catenin (red) and nuclear (blue) counterstaining.

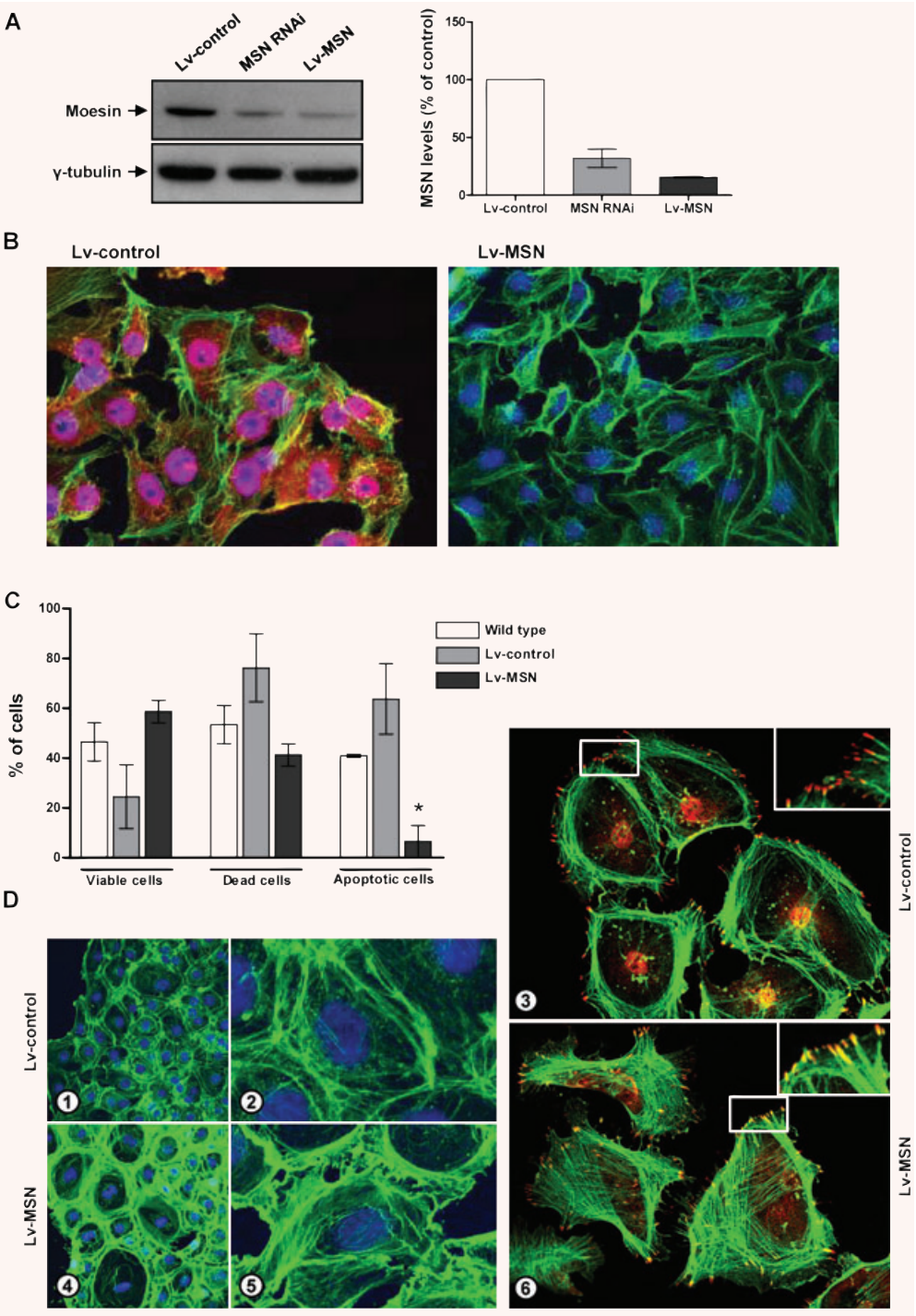

Fig. 4 Generation of a cell line stably expressing moesin shRNA. (**A**) Immunoblot analysis showing SU8686 cells stably transduced with shRNA for moesin (Lv-MSN) as compared to moesin siRNA-transfected (MSN RNAi) and scrambled shRNA (Lv-control) cells (left) and densitometric quantification of moesin down-regulation in SU8686 cancer cells (right). Data are shown as mean ± S.E.M. (**B**) Immunofluorescence analysis of Lv-MSN and Lv-control transduced SU8686 cells showing moesin (red), actin (green) and nuclear (blue) counterstaining. (**C**) Quantification of anoikis assay for Lv-MSN and Lv-control cells after detection of cell viability by FACS. Apoptotic cells were separated from the dead cell fraction. Data are shown as mean ± S.E.M. $^{*}P < 0.05$ compared to control cells. (**D**) Immunofluorescence analysis of actin cytoskeleton (green) using phalloidin staining, upon serum activation in Lv-control (1, 2) and Lv-MSN (4, 5) SU8686 cells. Vinculin staining (red) of Lv-control (3) and Lv-MSN (6) cells, demonstrating focal adhesion co-localization with radiating F-actin (green) stress fibre ends.

focal adhesions of Lv-MSN cells revealed increased co-localization with actin fibres compared to Lv-control cells (Fig. 4D-3, 6). It is therefore likely that moesin-regulated migratory and adhesion changes of pancreatic cancer cells are promoted through cytoskeleton re-organization.

Expression of moesin results in an 'anaplastic pattern of growth' of PDAC cells

In vivo, subcutaneous nude mouse tumours appeared earlier and grew faster in the Lv-MSN group compared to Lv-controls

(Fig. 5A). Tumour volume after 6 weeks was 3.0 ± 0.6 mm^3 for Lv-control and 8.75 ± 1.75 mm^3 for Lv-MSN ($P < 0.05$). Immunohistochemical evaluation of orthotopic tumours revealed strong expression of moesin in Lv-control tumours (Fig. 5B-1, 2) and faint staining in Lv-MSN tumours (Fig. 5B-3–5), as expected. Lv-control tumour cells displayed homogenous growth, with necrotizing areas within the tumour (Fig. 5B-1, 2). In contrast, Lv-MSN tumours developed duct-like structures (Fig. 5B-3–5).

Quantification of proliferation and microvessel density of orthotopic tumours revealed significantly higher number of microvessels (Fig. 5C-1) and a higher proliferation index (Fig. 5C-2) of Lv-MSN tumours compared to control tumours. Since in the subcutaneous and orthotopic model, no metastases were observed, intraportal injection of cancer cells was carried out next to evaluate the metastatic potential. Animals had to be sacrificed after 1 month due to the development of clinical symptoms of rapid tumour growth in mice of the Lv-MSN group. As expected, we identified large liver metastases in two of the three Lv-MSN injected mice. These metastatic tumours displayed duct-like structures with direct contact to the liver parenchyma without encapsulation (Fig. 5D-1–3). In contrast, neither gross nor micrometastases were found in Lv-control injected mice ($n = 3$), suggesting a comparably lower metastatic activity of moesin expressing pancreatic cancer cells.

For better evaluation of the growth differences of Lv-MSN and Lv-control tumours, we next analysed the distribution of the extracellular matrix (ECM) in *in vivo* grown tumours. Lv-control tumours demonstrated a poorly organized ECM, with weak expression of fibronectin-1 (Fig. 6A-1). In contrast, Lv-MSN tumours displayed well-developed and well-arranged ECM, with strong expression of fibronectin-1 in the basal parts of the duct-like structures (Fig. 6A-2).

Next, we analysed β-catenin, E-cadherin and N-cadherin distribution in Lv-MSN and Lv-control orthotopic tumours. Lv-control tumours displayed a more organized pattern of β-catenin expression (Fig. 6B-1) than tumours of Lv-MSN, where β-catenin distribution was cytoplasmic throughout the tumour tissue (Fig. 6B-2). In contrast, there was no difference in the expression and distribution of E-cadherin between Lv-control and Lv-MSN tumours (Fig. 6B-3, 4). In line with the *in vitro* results, we found strong expression of N-cadherin in all Lv-control tumours (Fig. 6B-5), and down-regulation in Lv-MSN tumour tissues (Fig. 6B-6), suggesting that moesin regulates expression of N-cadherin in SU8686 cells.

Finally, the growth pattern of *in vivo* tumours was compared to human pancreatic cancer tissues. In addition to the lack of moesin expression and the characteristic ECM distribution, several morphological similarities were clearly noticeable, such as cancerous ductal structures in Lv-MSN tumours which are also usually present in PDAC (Fig. 7). In contrast, Lv-control tumours, which express moesin, demonstrated a sarcomatoid type of growth. Chaotically, arranged large pleomorphic cells of these tumours did not build stroma, and formed large necrotic areas within the tissue (Fig. 7). These characteristics closely resemble the morphology of PAC (Fig. 7) and indicate the involvement of moesin in the anaplastic phenotype of pancreatic cancer.

We also analysed the expression of moesin in three recently engineered transgenic mouse models: the $P48^{+/Cre}$;$LSL\text{-}Kras^{G12D}$ mouse model, which is characterized by the development of PanIN lesions, ductal-type adenocarcinoma and metastasis [24]; and the Pdx^{-Cre};$CLEG2$;$Kras^{G12D}$ and Pdx^{-Cre};$CLEG2$ models, displaying undifferentiated/anaplastic growth patterns together with PanIN formation [23]. Interestingly, cancer cells of the $P48^{+/Cre}$;$LSL\text{-}Kras^{G12D}$ mouse, which demonstrated a more differentiated growth pattern, did not exhibit moesin expression. However, in areas where cancer cells displayed an anaplastic morphology, cancer cells were clearly moesin positive (Fig. 7). In line with this observation, anaplastic formations of Pdx^{-Cre};$CLEG2$;$Kras^{G12}$ pancreatic tissues strongly expressed moesin. Nevertheless, moesin was absent in surrounding PanIN lesions of the same tissue (Fig. 7). Pdx^{-Cre};$CLEG2$ mice developed undifferentiated solid tumours with predominantly monomorphic cells, which did not express moesin (Fig. 7). These undifferentiated monomorphic tumour areas were also seen in Pdx^{-Cre};$CLEG2$;$Kras^{G12}$ mice, which, like PanIN lesions, were moesin negative. These results suggest that moesin might play a specific role in neoplastic structures closely resembling human PAC.

Discussion

Moesin, a member of the ERM protein family, is involved in the association of the plasma membrane with the actin component of the cytoskeleton [6] and was preliminary isolated as a heparin-binding protein [29]. A conformational change induced by phosphorylation results in the active form of the protein [30], which binds actin and cell-type-dependent transmembrane proteins, such as CD44, CD43 and several I-CAMs [6] and, is thus involved in the pathogenesis of different malignancies.

The expression and localization of β-catenin strongly influences cytoskeleton reorganization during pancreatic tumourigenesis [27, 31, 32]. In this study, we demonstrated that β-catenin is co-expressed with moesin at the cell membrane and that silencing of moesin leads to cytoplasmic translocation of this protein. Membranous stabilization of β-catenin contributes to tumour suppression [31], therefore it could be hypothesized that expression of moesin reduces invasion of pancreatic cancer cells *via* maintaining membranous localization of β-catenin.

Expression of moesin has been suggested as a prognostic factor for different types of malignancies [28, 33, 34], and has previously also been evaluated in PDAC tissues [14]. In line with our observation, the published figures [14] demonstrate absence of moesin expression in cancer cells and strong staining in the stromal compartment. We now show that PAC was the only pancreatic malignancy with detectable moesin expression in the neoplastic cells. Despite the limited clinical experience with anaplastic pancreatic carcinoma, our data are in line with observations that anaplastic pancreatic cancers form large tumours often with central necrosis and limited desmoplasia that do not seem to aggressively invade surrounding structures. In addition, in relation

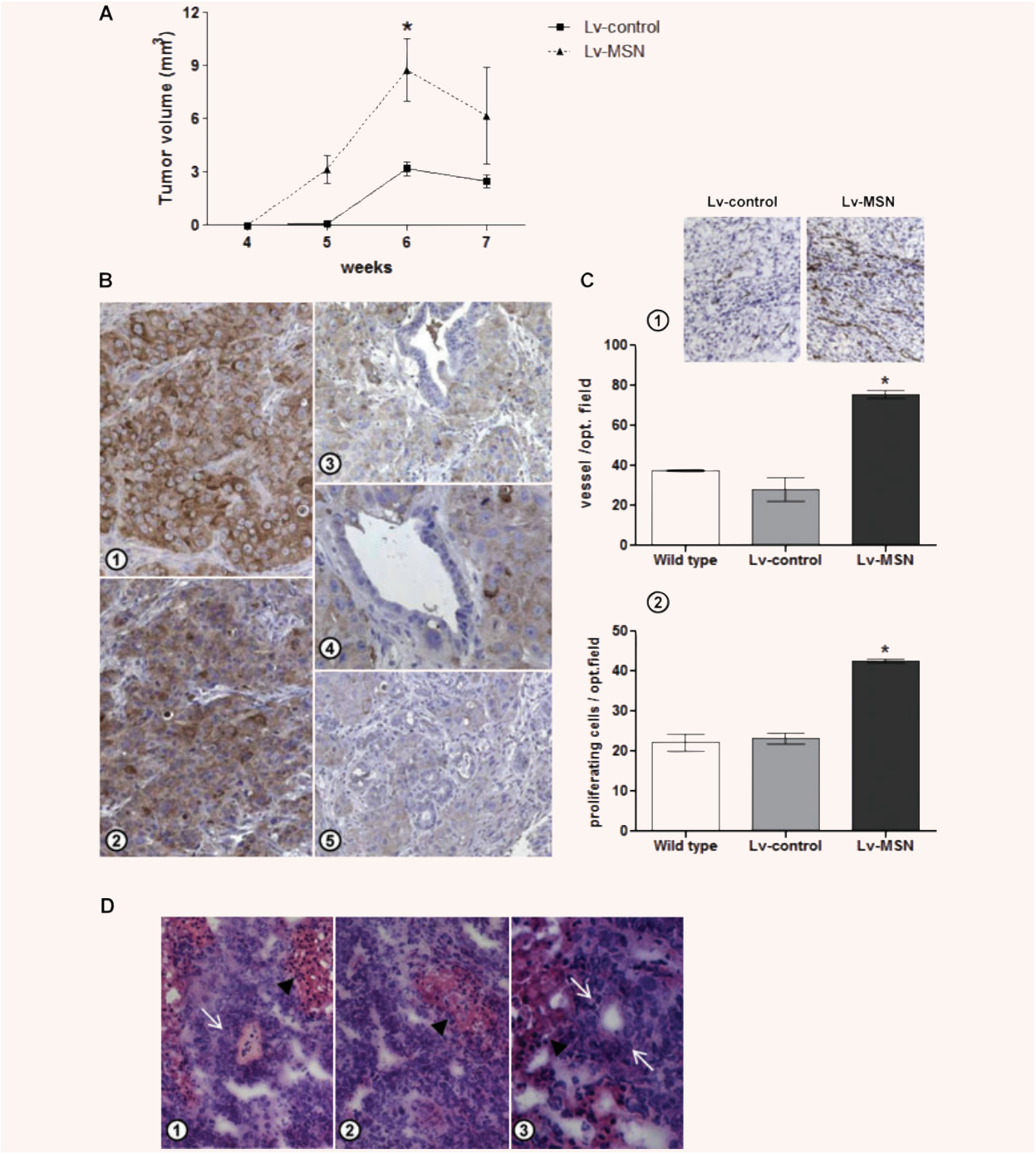

Fig. 5 Effects of moesin expression on *in vivo* tumourigenicity of pancreatic cancer cells. (**A**) Subcutaneous tumour growth of Lv-control and Lv-MSN clones in nude mice. Data are derived from three independent experiments and are presented as the mean tumour volume ± S.E.M. (**B**) Immunohistochemistry of Lv-control (1, 2) and Lv-MSN (3–5) tumours using a specific moesin antibody (20× magnification). (**C1–2**) Quantification of vessels and proliferating cells in control and Lv-MSN orthotopic tumours was performed using CD31 and Ki-67 immunostaining. Data are expressed as the mean of the number of vessels or proliferating cells per high-power field ± S.E.M. $*P < 0.05$ compared to control cells. (**D**) Haematoxylin and eosin staining of Lv-MSN liver metastases displaying multilayer cancer cell structures (white arrows) in the mouse liver tissue (black arrowheads) (20× magnification).

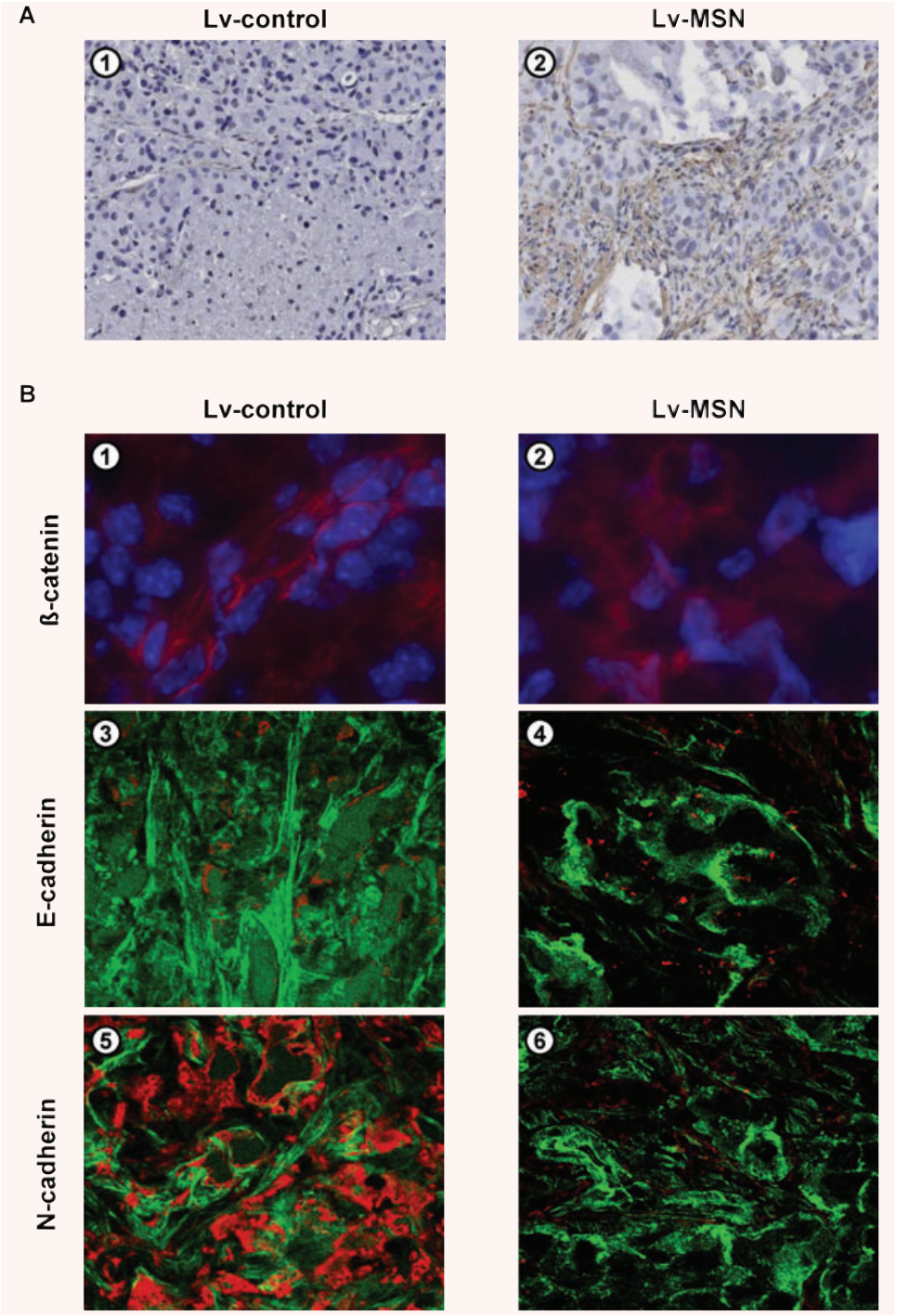

Fig. 6 Distribution of ECM and expression of EMT molecules in orthotopic nude mice tumours. (**A**) Immunohistochemistry using a specific fibronectin-1 antibody showing expression and organization of the ECM in Lv-MSN (2) and Lv-control tumours (1), (20× magnification). (**B**) Immunofluorescence staining of Lv-control and Lv-MSN tumours using β-catenin (1, 2), E-cadherin (3, 4) and N-cadherin (5, 6) antibodies (red). Phalloidin staining represents the actin cytoskeleton (green 3–6), nuclear counterstaining with DAPI (blue 1, 2).

to their size at presentation, these tumours seem to metastasize comparably later than PDAC. It could therefore be speculated that loss of moesin expression is one of the factors that results in increased invasiveness and metastasis of PDAC *in vivo*. Reconstitution of moesin expression might therefore prevent this invasive phenotype but on the other hand might result in an anaplastic growth pattern.

PDAC cells, which have high levels of ezrin, did not show any presence of moesin. Besides the evidence that moesin can be a marker of PAC, this finding indicates an essential difference

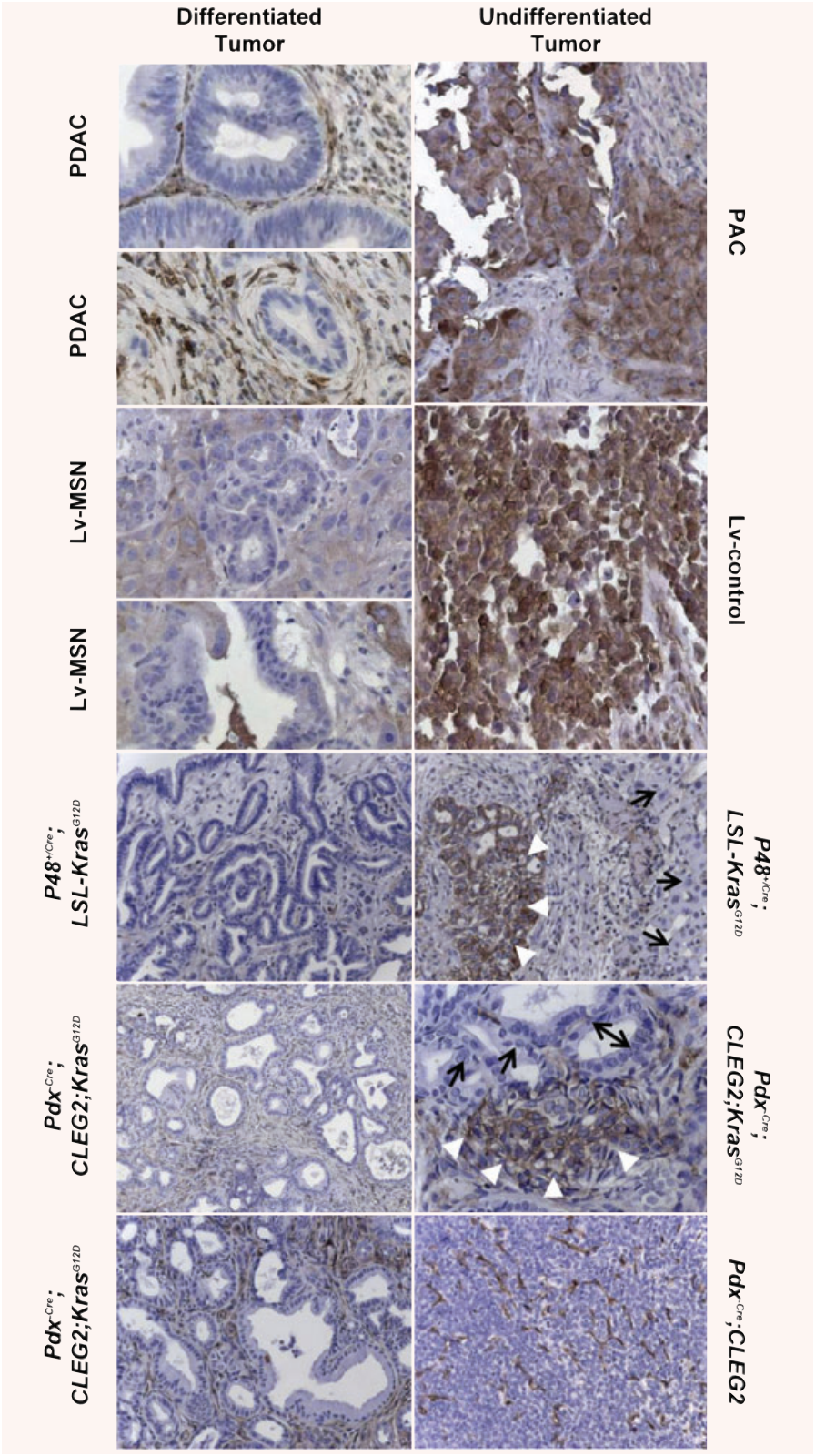

Fig. 7 Expression of moesin results in an 'anaplastic pattern of growth' of pancreatic cancer cells. Immunohistochemical staining of various human and mouse differentiated and undifferentiated pancreatic tumours with a specific moesin antibody. Moesin-positive anaplastic formations in transgenic mice tumours are marked with arrowheads. Arrows indicate liver cells in *P48$^{+/Cre}$;LSL-Kras^{G12D}* mouse metastatic tissue and moesin-negative PanIN lesions in *Pdx^{-Cre};CLEG2;Kras^{G12D}* mouse tumours.

between these two structurally related proteins. Moesin was equally absent in PDAC of all differentiation grades, including poorly differentiated (G3) tumours, suggesting a phenotype-specific role of moesin, rather than its involvement in de-differentiation processes.

Cultured PDAC cell lines represent an *in vitro* model of pancreatic cancer, and provide a useful tool for *in vitro* or *in vivo* evaluation of physiological and pathophysiological processes of cancer cells [35]. However, expression of moesin in PDAC cell lines obviously results in anaplastic characteristics rather than a ductal adenocarcinoma phenotype. Thus, the frequently used PDAC cells more closely represent PAC cells and it can be questioned, whether tumour models using these cell lines are relevant for PDAC.

PDAC as well as PAC might arise from PanIN lesions, and according to our observation, moesin might be a potential factor driving this process to anaplastic tumours. The reasons for the *de novo* moesin expression in long-term cultured PDAC cells are currently not known, as well as whether this *in vitro* transformation also occurs in PDAC tissues; however, we suggest that PAC cells derive either from PanIN [25] or from PDAC.

In conclusion, moesin expression is associated with an anaplastic phenotype of pancreatic cancer and may have important functions in the regulation of cellular architecture, migration, invasion and metastasis.

Acknowledgements

We thank Dr. Hubertus Schmitz-Winnenthal for kindly providing pPDAC cells and Dr. Thilo Welsch for the help in analysing focal adhesions (Department of General Surgery, University of Heidelberg). We would like to thank Drs. Mathias Hebrok and Marina Pasca di Magliano (Diabetes Center, Department of Medicine, University of California, San Francisco) for kindly providing *Pdx*$^{-Cre}$*; CLEG2; Kras*^{G12D} and *Pdx*$^{-Cre}$*; CLEG2* transgenic mice tissues. This project was supported in part by a doctoral scholarship of the Boehringer Ingelheim Fonds awarded to Ivane Abiatari.

References

1. **Welsch T, Kleeff J, Friess H.** Molecular pathogenesis of pancreatic cancer: advances and challenges. *Curr Mol Med*. 2007; 7: 504–21.
2. **Jones S, Zhang X, Parsons DW, *et al.*** Core signaling pathways in human pancreatic cancers revealed by global genomic analyses. *Science*. 2008; 321: 1801–6.
3. **Jemal A, Siegel R, Ward E, *et al.*** Cancer statistics, 2008. *CA Cancer J Clin*. 2008; 58: 71–96.
4. **Kleeff J, Michalski C, Friess H, *et al.*** Pancreatic cancer: from bench to 5-year survival. *Pancreas*. 2006; 33: 111–8.
5. **Hoorens A, Prenzel K, Lemoine NR, *et al.*** Undifferentiated carcinoma of the pancreas: analysis of intermediate filament profile and Ki-ras mutations provides evidence of a ductal origin. *J Pathol*. 1998; 185: 53–60.
6. **Tsukita S, Yonemura S, Tsukita S.** ERM proteins: head-to-tail regulation of actin-plasma membrane interaction. *Trends Biochem Sci*. 1997; 22: 53–8.
7. **Speck O, Hughes SC, Noren NK, *et al.*** Moesin functions antagonistically to the Rho pathway to maintain epithelial integrity. *Nature*. 2003; 421: 83–7.
8. **Miller KG.** A role for moesin in polarity. *Trends Cell Biol*. 2003; 13: 165–8.
9. **Pilot F, Philippe JM, Lemmers C, *et al.*** Spatial control of actin organization at adherens junctions by a synaptotagmin-like protein Btsz. *Nature*. 2006; 442: 580–4.
10. **Akisawa N, Nishimori I, Iwamura T, *et al.*** High levels of ezrin expressed by human pancreatic adenocarcinoma cell lines with high metastatic potential. *Biochem Biophys Res Commun*. 1999; 258: 395–400.
11. **Ohtani K, Sakamoto H, Rutherford T, *et al.*** Ezrin, a membrane-cytoskeletal linking protein, is involved in the process of invasion of endometrial cancer cells. *Cancer Lett*. 1999; 147: 31–8.
12. **Yeh TS, Tseng JH, Liu NJ, *et al.*** Significance of cellular distribution of ezrin in pancreatic cystic neoplasms and ductal adenocarcinoma. *Arch Surg*. 2005; 140: 1184–90.
13. **Hustinx SR, Fukushima N, Zahurak ML, *et al.*** Expression and prognostic significance of 14–3-3sigma and ERM family protein expression in periampullary neoplasms. *Cancer Biol Ther*. 2005; 4: 596–601.
14. **Torer N, Kayaselcuk F, Nursal TZ, *et al.*** Adhesion molecules as prognostic markers in pancreatic adenocarcinoma. *J Surg Oncol*. 2007; 96: 419–23.
15. **McClatchey AI.** Merlin and ERM proteins: unappreciated roles in cancer development? *Nature Rev*. 2003; 3: 877–83.
16. **Bretscher A, Edwards K, Fehon RG.** ERM proteins and merlin: integrators at the cell cortex. *Nat Rev Mol Cell Biol*. 2002; 3: 586–99.
17. **Hughes SC, Fehon RG.** Understanding ERM proteins – the awesome power of genetics finally brought to bear. *Curr Opin Cell Biol*. 2007; 19: 51–6.
18. **Erkan M, Kleeff J, Gorbachevski A, *et al.*** Periostin creates a tumor-supportive microenvironment in the pancreas by sustaining fibrogenic stellate cell activity. *Gastroenterology*. 2007; 132: 1447–64.
19. **Erkan M, Kleeff J, Esposito I, *et al.*** Loss of BNIP3 expression is a late event in pancreatic cancer contributing to chemoresistance and worsened prognosis. *Oncogene*. 2005; 24: 4421–32.
20. **Abiatari I, Kleeff J, Li J, *et al.*** Hsulf-1 regulates growth and invasion of pancreatic cancer cells. *J Clin Pathol*. 2006; 59: 1052–8.
21. **Michl P, Ramjaun AR, Pardo OE, *et al.*** CUTL1 is a target of TGF(beta) signaling that enhances cancer cell motility and invasiveness. *Cancer Cell*. 2005; 7: 521–32.
22. **Frisch SM, Francis H.** Disruption of epithelial cell-matrix interactions induces apoptosis. *J Cell Biol*. 1994; 124: 619–26.
23. **Pasca di Magliano M, Sekine S, Ermilov A, *et al.*** Hedgehog/Ras interactions regulate early stages of pancreatic cancer. *Genes Dev*. 2006; 20: 3161–73.

24. **Guerra C, Schuhmacher AJ, Canamero M, *et al.*** Chronic pancreatitis is essential for induction of pancreatic ductal adenocarcinoma by K-Ras oncogenes in adult mice. *Cancer Cell*. 2007; 11: 291–302.
25. **Bergmann F, Esposito I, Michalski CW, *et al.*** Early undifferentiated pancreatic carcinoma with osteoclastlike giant cells: direct evidence for ductal evolution. *Am J Surg Pathol*. 2007; 31: 1919–25.
26. **Nakajima S, Doi R, Toyoda E, *et al.*** N-cadherin expression and epithelial-mesenchymal transition in pancreatic carcinoma. *Clin Cancer Res*. 2004; 10: 4125–33.
27. **Brabletz T, Jung A, Spaderna S, *et al.*** Opinion: migrating cancer stem cells – an integrated concept of malignant tumour progression. *Nat Rev Cancer*. 2005; 5: 744–9.
28. **Kobayashi H, Sagara J, Kurita H, *et al.*** Clinical significance of cellular distribution of moesin in patients with oral squamous cell carcinoma. *Clin Cancer Res*. 2004; 10: 572–80.
29. **Lankes W, Griesmacher A, Grunwald J, *et al.*** A heparin-binding protein involved in inhibition of smooth-muscle cell proliferation. *Biochem J*. 1988; 251: 831–42.
30. **Bretscher A, Reczek D, Berryman M.** Ezrin: a protein requiring conformational activation to link microfilaments to the plasma membrane in the assembly of cell surface structures. *J Cell Sci*. 1997; 110: 3011–8.
31. **Kreimann EL, Morales FC, de Orbeta-Cruz J, *et al.*** Cortical stabilization of beta-catenin contributes to NHERF1/EBP50 tumor suppressor function. *Oncogene*. 2007; 26: 5290–9.
32. **Heiser PW, Cano DA, Landsman L, *et al.*** Stabilization of beta-catenin induces pancreas tumor formation. *Gastroenterology*. 2008; 135: 1288–300.
33. **Belbin TJ, Singh B, Smith RV, *et al.*** Molecular profiling of tumor progression in head and neck cancer. *Arch Otolaryngol Head Neck Surg*. 2005; 131: 10–8.
34. **Tokunou M, Niki T, Saitoh Y, *et al.*** Altered expression of the ERM proteins in lung adenocarcinoma. *Lab Invest*. 2000; 80: 1643–50.
35. **Ulrich AB, Schmied BM, Standop J, *et al.*** Pancreatic cell lines: a review. *Pancreas*. 2002; 24: 111–20.